QUANTITATIVE FINANCE
RESEARCH CENTRE

UNIVERSITY OF
TECHNOLOGY SYDNEY

QUANTITATIVE FINANCE RESEARCH CENTRE

Research Paper 388 January 2018

On Numerical Methods for Spread Options

Mesias Alfeus and Erik Schlögl

ISSN 1441-8010 www.qfrc.uts.edu.au

On Numerical Methods for Spread Options

Mesias Alfeus* and Erik Schlögl†

January 11, 2018

Abstract

Spread options are multi-asset options whose payoffs depend on the difference of two underlying financial variables. In most cases, analytically closed form solutions for pricing such payoffs are not available, and the application of numerical pricing methods turns out to be non-trivial. We consider several such non-trivial cases and explore the performance of the highly efficient numerical technique of Hurd and Zhou (2010), comparing this with Monte Carlo simulation and the lower bound approximation formula of Caldana and Fusai (2013). We show that the former is in essence an application of the two–dimensional Parseval Identity.

As application examples, we price spread options in a model where asset prices are driven by a multivariate normal inverse Gaussian (NIG) process, in a three-factor stochastic volatility model, as well as in examples of models driven by other popular multivariate Lévy processes such as the variance Gamma process, and discuss the price sensitivity with respect to volatility. We also consider examples in the fixed–income market, specifically, on cross–currency interest rate spreads and on LIBOR/OIS spreads. In terms of FFT computation, we have used the FFTW library (see Frigo and Johnson (2010)) and we document appropriate usage of this library to reconcile it with the MATLAB *ifft2* counterpart.

1 Introduction

Spread options are multi-asset financial securities that are quite common in for instance fixed-income markets, foreign exchange markets and commodity derivatives markets, just to mention a few. By definition, a spread option is an option written on the difference of two financial variables. For example, in the fixed-income market a spread option might be a call option on the difference between LIBORs of different maturities.

Pricing spread options with non-zero strikes is typically not amenable to closed form (analytical) solutions, and the goal of this paper is to investigate numerical methods for spread options, building on the innovative approach of Hurd and Zhou (2010), i.e., a

*University of Technology Sydney, Australia
e-mail: Mesias.Alfeus@student.uts.edu.au
†University of Technology Sydney, Australia
e-mail: Erik.Schlogl@uts.edu.au

direct extension to multi-asset pricing of the fast Fourier transform (FFT), an approach which was introduced to finance in the work of Carr and Madan (1999). This method is applicable to models in which the joint characteristic function of the price of the underlying asset is known explicitly. We shall explore various asset dynamics, driven by Geometric Brownian motion (GBM), by a stochastic volatility (SV) model and by the more general Lévy models. In Lévy models, we focus on Variance Gamma (VG) and Normal Inverse Gaussian (NIG) driving processes, which are commonly used in market risk applications.

To the best of our knowledge, the first study to apply FFT pricing techniques to correlation options and spread options was Dempster and Hong (2002). In the case for spread options, Dempster and Hong approximated the exercise region through a combination of rectangular strips, thereby attempting to account for singularities in the transform variables. They then applied FFT techniques on a regularised region to derive the upper and lower bounds for the spread option value. Spread options have an exercise region with non-linear edge and applying the methodology of Dempster and Hong can be computationally expensive. As an alternative to deriving the analytic approximation of the 2-dimensional exercise region, Hurd and Zhou (2010) propose a more suitable version of FFT algorithm for pricing options in two and higher dimensions, which is based on square integrable integral formulae for the payoff function.

The key idea underpinning Hurd and Zhou methodology is to perform the Fourier transform of the spread options payoff, assuming the knowledge of the model (joint) characteristic function, which is finally expressed as a pointwise multiplication of the characteristic function and the complex gamma function. This is essentially a two–dimensional Fourier transform of a payoff function and in this way, it converges rapidly to the true value. The advantage of this method is that it does not suffer from the curse of dimensionality. This method has been proven to have $O(N^2 \log N)$ complexity (in grid size N), in comparison to $O(N^4)$ of a conventional Fourier transform and hence it is understood to be the most efficient method in the literature for spread option valuation. We will consider this method both in equity and in fixed-income markets. In each case, the method is compared to Monte Carlo simulation and the lower bound approximation method of Caldana and Fusai (2013).

The first contribution of this paper is the derivation of a two-dimensional version of Parseval's Identity of the Mellin transform, and showing that the method of Hurd and Zhou (2010) is essentially an application of this identity. Secondly, we document how to reconcile a (much faster) FFT implementation in C++ using the *Fastest Fourier Transform in the West* (FFTW) library with results obtained using the popular MATLAB *ifft2* routine. Thirdly, we provide additional application examples, both in terms of driving dynamics (specifically, normal inverse Gaussian) and in terms of markets (considering options on

spreads between interest rates in different currencies, and between LIBOR and OIS).

The rest of the paper is organised as follows. Section 1 describes the spread pricing problem. Section 2 is devoted to a discussion of Fourier Transform techniques in both one and two dimensions. For the reader's convenience, we give an overview of the Carr and Madan (1999) FFT method of derivative pricing. In that section, we also look at Parseval's Identity[1] in one dimension and prove its validity in the two dimensional case. Section 3 discusses different pricing models in terms of their joint characteristic functions, setting up the modelling context for the spread option pricing case studies in the subsequent sections. In Section 4, we price spread option in the equity market, presenting numerical pricing results and a sensitivity analysis with respect to volatility. An implementation example for spread options in the fixed-income market follows in Section 5. There we consider two examples, the first being a spread option between two LIBORs belonging to different currencies, and the second being an option on the LIBOR-OIS spread. Section 6 concludes.

1.1 The pricing problem

Fix the real-time horizon $\mathbb{T}$ and consider a probability space $\left(\Omega, \mathcal{F}, \mathbb{P}, (\mathcal{F}_t)_{t<T<\mathbb{T}}\right)$ defined in the usual sense.

Consider an European spread option between stock price processes $S_1 = \{S_1(t)\}_{0\leq t\leq T}$ and $S_2 = \{S_2(t)\}_{0\leq t\leq T}$ with maturity time T and exercise price K. The payoff is given by

$$\mathcal{S}_T(S_1, S_2, K) = \max\{S_1(T) - S_2(T) - K, 0\}, \tag{1.1}$$

and under a risk-neutral measure[2] $\mathbb{Q}$ its value at time t is given by

$$\mathcal{S}_t(S_1, S_2, K) = e^{-r(T-t)}\mathbb{E}^{\mathbb{Q}}\left[(S_1(T) - S_2(T) - K)^+ \middle| \mathcal{F}_t\right]. \tag{1.2}$$

If the logarithmic return for individual assets is assumed to be normally distributed (as an example), the log return distribution of the difference is not known. This makes the pricing problem not amenable to closed form solutions if the strike K is non-zero. Dempster and Hong (2002) similarly pointed out that the main obstacle to a "clean" pricing methodology lies in the lack of knowledge about the distribution of the difference between two non-trivially correlated stochastic processes. Thus one must resort to numerical methods such as Monte Carlo or other numerical integration methods. Under

[1] Sometimes called the Plancherel–Parseval Identity

[2] Specifically: Under the risk–neutral measure associated with taking the continuously compounded savings account as the numeraire, and (for expositional simplicity) assuming a constant interest rate r.

the classical assumptions of Black and Scholes (1973), Kirk (1995) derived an approximation formula for spread options which is widely applied in practice but not as accurate as desired.

Departing from log-normality assumptions typically exacerbates the difficulty of the problem. Although Monte Carlo method is always an alternative solution to solving many problems, it is computationally expensive. Other numerical methods (e.g. finite difference methods) tend to suffer from the curse of dimensionality. The method which is widely seen to be effective in this context is the fast Fourier transform (FFT), as introduced to option pricing by Carr and Madan (1999). The key prerequisite for the application of this method is the knowledge of the characteristic function of the asset return. Eberlein et al. (2010) discuss further technical conditions and provide a number of application examples. For the multi-asset case, the first Fourier Transform implementation is due to Dempster and Hong (2002). This was subsequently extended by Hurd and Zhou (2010) in order to improve computational efficiency, and this forms the starting point for this note.

2 Fourier Transform method

In this section, the concept of Fourier transform is reviewed.

Definition 2.1 (Fourier Transform)**.** *Let $f : \mathbb{R} \to \mathbb{R}$ be a piecewise continuous function such $f \in L^1(\mathbb{R}) \cap L^2(\mathbb{R})$[3]. The Fourier transform of f is defined as follows:*

$$\mathcal{F}[f](u) := \hat{f}(u) := \int_{-\infty}^{\infty} e^{\mathrm{i}ux} f(x)dx, \ \mathrm{i} = \sqrt{-1}, \ \textit{and} \ \forall u \in \mathbb{R}. \tag{2.1}$$

The inverse of a Fourier transform is given by the *Fourier inversion formula:*

$$\mathcal{F}^{-1}[\hat{f}](x) = \frac{1}{2\pi} \int_{-\infty}^{\infty} e^{-\mathrm{i}ux} \hat{f}(x)dx. \tag{2.2}$$

In option pricing theory, usually an interesting case is when f is the Lebesgue density function of a particular probability distribution. In that case, the Fourier transform of f boils down to the characteristic function of that distribution, i.e.

$$\mathcal{F}[f](u) := \Phi(u),$$

which often simplifies the pricing problems, as in many cases it is much more tractable to work with characteristic functions instead of distribution functions. Moreover, one is

[3] A space of absolutely and square integrable functions

able to recover the distribution function from the characteristic function via the Fourier inversion formula in (2.2).

The complex conjugate of a Fourier transform function (real-valued) is defined by

$$\overline{\hat{f}(u)} = \hat{f}(-u),$$

and it is very common in the application of Parseval's Identity.

The relation in Definition 2.1 can be generalized by considering $a, b \in \mathbb{R}$ such that $a < b$: Define a strip

$$\mathsf{S} = \{u \in \mathbb{C} : a < \text{Im}\{u\} < b\},$$

to extend the domain for the transform variable u to the complex plane. Then Definition 2.1 can be extended to the entire complex plane:

$$\mathcal{F}[f](u) := \hat{f}(u) := \int_{-\infty}^{\infty} e^{iux} f(x)dx, \; u \in \mathsf{S}. \tag{2.3}$$

A useful result for option pricing using Fourier transform techniques is Parseval's Identity, first applied (in the one-dimensional case) by Lewis (2001).

Theorem 2.1 (Parseval's Identity in one dimension)**.** *Let $f, g \in L^2$, then*

$$\begin{aligned}\int_{-\infty}^{\infty} f(s)\overline{g(s)}ds &= \frac{1}{2\pi}\int_{-\infty}^{\infty} \hat{f}(u)\overline{\hat{g}(u)}du \\ &= \frac{1}{2\pi}\int_{-\infty}^{\infty} \hat{f}(u_r + \mathrm{i}u_i)\overline{\hat{g}(u_r + \mathrm{i}u_i)}du_r,\end{aligned}$$

where special care needs to be taken to make sure the integrand, i.e., the product of functions f and g, is either continuous, or at most discontinuous at only countably many points $\Im\{u\} = u_i$[4]*.*

To see the application of this theorem to option pricing, let q be the underlying density function of the probability distribution of log asset price and P be the option payoff at maturity time T, then the time $t = 0$ value of the option is given by

$$\begin{aligned}\mathbb{V}_0 = e^{-rT}\mathbb{E}[P(T) \mid \mathcal{F}_0] &= e^{-rT}\int_{-\infty}^{\infty} P(s)q(s)ds \\ &= \frac{e^{-rT}}{2\pi}\int_{-\infty}^{\infty} \hat{P}(u)\hat{q}(-u)du \\ &= \frac{e^{-rT}}{2\pi}\int_{-\infty}^{\infty} \hat{P}(u)\Phi(-u)du.\end{aligned}$$

[4]With notation $u_i = \Im\{u\}$ and $u_r = \Re\{u\}$.

2.1 Fast Fourier transform in one-dimension

This section reviews the method of Carr and Madan (1999), who transform the call option payoff with respect to the log-asset price to make it amenable to the application of FFT techniques.

Let $N = 2^m$ for some $m \in \mathbb{Z}^+$. N needs to be a power of 2 because FFT procedure splits the problem recursively into two halves. Now define an N vector of real numbers $h = (h_0, h_1, \cdots, h_{N-1})$. Then the discrete Fourier Transform of h is another N-vector given by

$$\hat{h}_n = \sum_{j=0}^{N-1} \alpha_n^j h_j,$$

and the inverse discrete Fourier transform is given by

$$\mathcal{F}^{-1}[\hat{h}]_j = \frac{1}{N} \sum_{n=0}^{N-1} \alpha_j^n \hat{h}_n := h_j,$$

where

$$\alpha_n^j = e^{\mathrm{i}\frac{2\pi}{N}jn}$$

are elements in an $N \times N$ matrix.

The computation of $\hat{h}$ requires N^2 multiplications and $N^2 - N$ additions. However, the fast Fourier technique only need $\frac{1}{2}N \log_2 N$ operations, which means that the speed is tremendously increased, see also Carr and Madan (1999).

Consider a European call with the maturity time T and the strike price K, which is written on a stock whose price process is S_t, i.e, the payoff expressed in term of log strike price is given by

$$P(k) = \max\{e^x - e^k, 0\} \text{ where } x = \log S(T), \text{ and } k = \log K. \tag{2.4}$$

The price of this call option is then given by

$$\mathbb{V}(k) = e^{-rT}\mathbb{E}[P(k)] = e^{-rT} \int_k^\infty (e^x - e^k) q_T(x) dx, \tag{2.5}$$

where q_T is the risk-neutral density of log asset price at time T.

As the strike goes to zero, a position in the call option on the (non-dividend–paying) asset becomes equivalent to holding the asset itself, so

$$e^{-rT} \lim_{k \to -\infty} \int_k^\infty (e^x - e^k) q_T(x) dx \to S_0,$$

This means that $\mathbb{V} \notin L^2$ (see Carr and Madan (1999)) and Fourier transform techniques

or the Parseval's Identity are not applicable in this case. To avoid this problem, Carr and Madan (1999) chose $\alpha > 0$, a dampening factor to enforce integrability, modifying the call price function to

$$\tilde{\mathbb{V}}(k, \alpha) = e^{\alpha k}\mathbb{V}(k). \tag{2.6}$$

Taking the Fourier transform of the modified call function gives

$$\begin{aligned}\mathcal{F}[\tilde{\mathbb{V}}(k,\alpha)](u) = \int_{-\infty}^{\infty} e^{\mathrm{i}uk}\tilde{\mathbb{V}}(k,\alpha)dk &= \int_{-\infty}^{\infty} e^{(iu+\alpha)k}\mathbb{V}(k)dk \\ &= e^{-rT}\int_{-\infty}^{\infty} q_T(s)ds \int_{-\infty}^{s} e^{\mathrm{i}uk}(e^{s+\alpha k} - e^{(1+\alpha)k})q_T(s)dk \\ &= \frac{e^{-rT}\Phi(u - \mathrm{i}(\alpha+1))}{\alpha^2 + \alpha - u^2 + \mathrm{i}u(2\alpha+1)}.\end{aligned}$$

Finally, to get the call price function $\mathbb{V}(k)$, perform the Fourier inversion, i.e.

$$\mathbb{V}(k) = \frac{1}{2\pi}\int_{-\infty}^{\infty} e^{-(\mathrm{i}u+\alpha)k}\mathcal{F}[\tilde{\mathbb{V}}(k,\alpha)](u)du = \frac{e^{-\alpha k}}{2\pi}\int_{-\infty}^{\infty} e^{-\mathrm{i}uk}\mathcal{F}[\tilde{\mathbb{V}}(k,\alpha)](u)du.$$

To approximate this integral, use the Trapezoidal Rule (or some other rule such Simpson's rule) using interval width Δu to get

$$\mathbb{V}(k_i) \approx \Delta u\frac{e^{-\alpha k_i}}{2\pi}\sum_{j=0}^{N-1} e^{-\mathrm{i}k_i u_j}\mathcal{F}[\tilde{\mathbb{V}}(k_j,\alpha)](u_j),\ i = 0, 1, \cdots, N-1,$$

where the grid points are defined by

$$\begin{cases} k_i = -\frac{1}{2}N\Delta k + i\Delta k, & i = 0, 1, \cdots, N-1, \\ u_j = -\frac{1}{2}N\Delta u + j\Delta u, & j = 0, 1, \cdots, N-1, \end{cases}$$

and Δu and Δk are chosen such that they satisfy the so called Nyquist criterion:

$$\Delta k\Delta u = \frac{2\pi}{N}. \tag{2.7}$$

Then the above numerical approximation can be expressed as

$$\mathbb{V}(k_i) \approx \Delta u\frac{e^{-\alpha k_i}}{2\pi}\sum_{j=0}^{N-1}(-1)^{i+j}e^{-\mathrm{i}\frac{2\pi}{N}ij}\mathcal{F}[\tilde{\mathbb{V}}(k_j,\alpha)](u_j),\ i = 0, 1, \cdots, N-1, \tag{2.8}$$

2.2 Fourier transform in two-dimensions

The two dimensional Fourier transform of $f(x_1, x_2)$ is given by

$$\mathcal{F}\{f(x_1,x_2)\}(u_1,u_2) = \hat{f}(u_1,u_2) = \int_{-\infty}^{\infty}\int_{-\infty}^{\infty} f(x_1,x_2)e^{-\mathrm{i}(u_1x_1+u_2x_2)}dx_1dx_2, \tag{2.9}$$

and the corresponding inversion formula is given by

$$\mathcal{F}^{-1}\{\hat{f}(u_1,u_2)\}(x_1,x_2) = f(x_1,x_2) = \frac{1}{4\pi^2}\int_{-\infty}^{\infty}\int_{-\infty}^{\infty} \hat{f}(u_1,u_2)e^{\mathrm{i}(u_1x_1+u_2x_2)}du_1du_2. \tag{2.10}$$

Theorem 2.2 (Parseval's Identity in two dimensions)**.** *Suppose* $\hat{f}(x_1, x_2)$ *and* $\hat{g}(x_1, x_2)$ *exist. Then*

$$\int_{-\infty}^{\infty}\int_{-\infty}^{\infty} f(x_1,x_2)\overline{g(x_1,x_2)}dx_1dx_2 = \frac{1}{4\pi^2}\int_{-\infty}^{\infty}\int_{-\infty}^{\infty} \hat{f}(u_1,u_2)\overline{\hat{g}(u_1,u_2)}du_1du_2. \tag{2.11}$$

Proof. From the Fubini Theorem, we know that

$$\int_{-\infty}^{\infty}\int_{-\infty}^{\infty} f(x_1,x_2)\hat{g}(x_1,x_2)dx_1dx_2 = \int_{-\infty}^{\infty}\int_{-\infty}^{\infty} \hat{g}(x_1,x_2)f(x_1,x_2)dx_1dx_2.$$

Since

$$g(x_1,x_2) = \frac{1}{4\pi^2}\int_{-\infty}^{\infty}\int_{-\infty}^{\infty} \hat{g}(u_1,u_2)e^{\mathrm{i}(u_1x_1+u_2x_2)}du_1du_2,$$

then we have

$$\begin{aligned}
&\int_{-\infty}^{\infty}\int_{-\infty}^{\infty} f(x_1,x_2)\overline{g(x_1,x_2)}dx_1dx_2 \\
=&\frac{1}{4\pi^2}\int_{-\infty}^{\infty}\int_{-\infty}^{\infty} f(x_1,x_2)\left\{\int_{-\infty}^{\infty}\int_{-\infty}^{\infty}\overline{\hat{g}(u_1,u_2)}e^{-\mathrm{i}(u_1x_1+u_2x_2)}du_1du_2\right\}dx_1dx_2 \\
=&\frac{1}{4\pi^2}\int_{-\infty}^{\infty}\int_{-\infty}^{\infty}\left\{\int_{-\infty}^{\infty}\int_{-\infty}^{\infty} f(x_1,x_2)e^{-\mathrm{i}(u_1x_1+u_2x_2)}dx_1dx_2\right\}\overline{\hat{g}(u_1,u_2)}du_1du_2 \\
=&\frac{1}{4\pi^2}\int_{-\infty}^{\infty}\int_{-\infty}^{\infty} \hat{f}(u_1,u_2)\overline{\hat{g}(u_1,u_2)}du_1du_2.
\end{aligned}$$

□

A more general Fourier–Mellin transform in two dimension was first derived by Sharma and Dolas (2016). Parseval's Identity brings FFT option pricing into a framework where the payoff function is expressed explicitly. Though they do not reference Parseval's Identity, this is in essence the idea of Hurd and Zhou (2010):

The payoff function in Equation (1.1) can be re-written as

$$\mathcal{S}_T(S_1, S_2, K) = K \max\left\{\frac{S_1(T)}{K} - \frac{S_2(T)}{K} - 1, 0\right\} = K \max\{e^{x_1} - e^{x_2} - 1, 0\}. \quad (2.12)$$

Let $X_{1t} = \log\left(\frac{S_1(T)}{K}\right)$ and $X_{2t} = \log\left(\frac{S_2(T)}{K}\right)$ with $X_{10} = x_1$ and $X_{20} = x_2$. Define

$$P(x_1, x_2) = \max\{e^{x_1} - e^{x_2} - 1, 0\}, \quad (2.13)$$

so that (2.12) becomes

$$\mathcal{S}_T(S_1, S_2, K) = KP(x_1, x_2) := g(x_1, x_2). \quad (2.14)$$

The 2-dimensional Fourier transform of the payoff function (2.13) is given by

$$g(x_1, x_2) = \frac{1}{4\pi^2}\int_{-\infty}^{\infty}\int_{-\infty}^{\infty}\hat{g}(u_1, u_2)e^{\mathrm{i}(u_1x_1+u_2x_2)}du_1du_2 \quad (2.15)$$

$$= \frac{1}{4\pi^2}\frac{\Gamma((\epsilon_1 + \mathrm{i}x_1) + (\epsilon_2 + \mathrm{i}x_2) - 1)\Gamma(-(\epsilon_2 + \mathrm{i}x_2))}{K^{(\epsilon_1+\mathrm{i}x_1)+(\epsilon_2+\mathrm{i}x_2)}\Gamma((\epsilon_1 + \mathrm{i}x_1) + 1)}, \quad (2.16)$$

for some $\epsilon_2 > 0$ and $\epsilon_1 + \epsilon_2 < -1$ and $[\epsilon_1 + \mathrm{i}x_1, \epsilon_2 + \mathrm{i}x_2] \in \mathcal{S}_W$, a strip in the complex z-plane. $\Gamma(z)$ is the complex gamma function defined by the integral

$$\Gamma(z) = \int_{\mathbb{R}^+} e^{-t}t^{z-1}dt, \ \mathrm{Re}(z) > 0,$$

and the two-dimensional strip $\mathsf{S}^2 := \{(u_1, u_2) \in \mathsf{S} \times \mathsf{S}\}$, where S is defined as in Equation (2.3).

The joint characteristic function of X_{1t} and X_{2t} is given by

$$\varphi(u_1, u_2) = \mathbb{E}\left[e^{\mathrm{i}u_1X_{1T}+\mathrm{i}u_2X_{2T}}\right] = e^{\mathrm{i}u_1x_1+\mathrm{i}x_2u_2}\Phi(u_1, u_2), \quad (2.17)$$

where $\Phi(u_1, u_2)$ is the joint characteristic function for$X_{1T} - x_1$ and $X_{2T} - x_2$.

Suppose $q_T(x_1, x_2)$ is the underlying density of the probability distribution of log asset price. Then spread option value is given by

$$V_0 = e^{-rT}\mathbb{E}^{\mathbb{Q}}\left[(e^{x_1} - e^{x_2} - K)^+\right] \quad (2.18)$$

$$= e^{-rT}\int_{-\infty}^{\infty}\int_{-\infty}^{\infty}q_T(x_1, x_2)g(x_1, x_2)dx_1dx_2 \quad (2.19)$$

In order to deal with convergence problems we can also allow the variable in the Fourier transform to be a complex number. Thus if we integrate along a some strip $\mathcal{S}_X$ in the

Algorithm 1: FFT algorithm for Spread Option pricing along the lines of Hurd and Zhou (2010)

2-D FFT $(N, \overline{u}, \epsilon)$;
Input : N, a power of two; $\overline{u}$, truncation width; ϵ, damping factor.
Define : $u(k) = (u_1(k_1), u_2(k_2))$ and $x(l) = (x_1(l_1), x_2(l_2))$
Set $X_0 = \left[\log\left(\frac{S_1}{K}\right), \log\left(\frac{S_2}{K}\right)\right] \in x(l)$
forall $k, l \in \{1, \cdots, N-1\}^2$ **do**
  $H(k) = (-1)^{k_1+k_2}\Phi(u(k) + i\epsilon)\hat{P}(u(k) + i\epsilon)$;
  $C(l) = (-1)^{l_1+l_2}e^{-rT}\left(\frac{\eta N}{2\pi}\right)^2 e^{-\epsilon x(l)'}$;
end
$V = \mathcal{R}_e(C \times \text{ifft2}(H))$ /* with $O(N^2 \log N)$ complexity*/
$P \leftarrow K \times V$ /* using an efficient interpolation technique*/;
Output: P

complex plane parallel to the real axis and having constant positive imaginary part, i.e. in strip $\mathcal{S}_W$, the integrand above will have a damping factor which may help to integrate legally. Therefore, we let $u_1 = \epsilon_1 + \mathrm{i}z_1$ and $u_2 = \epsilon_2 + \mathrm{i}z_2$. Then, by Parseval's Identity, (2.19) becomes

$$\begin{aligned}\int_{-\infty}^{\infty}\int_{-\infty}^{\infty} q_T(x_1, x_2)g(x_1, x_2)dx_1dx_2 &= \frac{1}{4\pi^2}\int_{-\infty}^{\infty}\int_{-\infty}^{\infty}\overline{\hat{q}_T(u_1, u_2)}\hat{g}(u_1, u_2)du_1du_2 \\ &= \frac{1}{4\pi^2}\int_{-\infty}^{\infty}\int_{-\infty}^{\infty}\hat{q}_T(-u_1, -u_2)\hat{g}(u_1, u_2)du_1du_2 \\ &= \frac{1}{4\pi^2}\int_{-\infty}^{\infty}\int_{-\infty}^{\infty}\Phi(-u_1, -u_2)\hat{g}(u_1, u_2)du_1du_2\end{aligned} \tag{2.20}$$

$\Phi(-u_1, -u_2)$ will only exist if $u_1, u_2 \in \mathcal{S}_X^*$, the reflection of $\mathcal{S}_X$ on real axis. In fact we need to ensure that $u_1, u_2 \in \mathcal{S}_X^* \cap \mathcal{S}_W$, see also Lewis (2001), p. 12.

This two-dimensional Fourier inversion integral can be well approximated (numerically) by two-dimensional fast Fourier transform. This approach does not require the approximation of the exercise region by the use of rectangular strips,[5] which is computationally intensive, making this method more efficient.

Now compute this double sum over the lattice (given N and $\overline{u}$):

$$\begin{cases} u(k) =: (u_1(k_1), u_2(k_2)) = \{\left(-\frac{1}{2}N\eta + i\eta k_1, -\frac{1}{2}N\eta + i\eta k_2\right) | k_1, k_2 = 0, 1, \cdots, N-1\} \\ x(l) =: (x_1(l_1), x_2(l_2)) = \{\left(-\frac{1}{2}N\eta^* + i\eta^* l_1, -\frac{1}{2}N\eta^* + i\eta^* l_2\right) | l_1, l_2 = 0, 1, \cdots, N-1\}, \end{cases}$$

where the lattice spacing η is given by $\eta = \frac{2\overline{u}}{N}$ and the reciprocal lattice for real-spacing η^* satisfies the Nyquist criterion, i.e. $\eta^* = \frac{2\pi}{N\eta} = \frac{\pi}{\overline{u}}$.

Choose $X_0 = (X_{10}, X_{20})$ in a such a way that it falls on a real-grid spacing, i.e. $X_0 \in x$,

[5] as proposed by Dempster and Hong (2002)

Table 1: Characteristic functions for the underlying models

Driving model	$\Phi(u;T)$
GBM	$\exp\left(iu\left(rTe-\frac{\sigma^2 T}{2}\right)'-\frac{u\Sigma u'T}{2}\right)$
3-SV	$\exp\left(\left(\frac{2\zeta(1-e^{-\theta T})}{2\theta-(\theta-\gamma)(1-e^{-\theta T})}\right)\nu_0+iu(re-\delta)'T-\frac{\kappa\mu}{\sigma_\nu^2}\Gamma\right)$
VG	$\left(\frac{1}{1-iu_1\theta_1\nu-iu_2\theta_2\nu+\nu u'\Sigma u/2}\right)^{\frac{T}{\nu}}$
NIG	$\exp\left(\mathrm{i}u'\mu T+\delta T\left[\sqrt{\alpha^2-\beta\Delta\beta'}-\sqrt{\alpha^2-(\beta+iu)\Delta(\beta+iu)'}\right]\right)$

so (2.20) can be numerically approximated follows:

$$\begin{aligned}
\mathbb{V}_t(x_1,x_2) &\approx \frac{e^{-r(T-t)}}{4\pi^2}\sum_{k_1=0}^{N_1}\sum_{k_1=0}^{N_1} e^{\mathrm{i}(u(k)+\mathrm{i}\epsilon)x(l)'}\hat{P}(u(k)+\mathrm{i}\epsilon)\Phi(u(k)+\mathrm{i}\epsilon)\\
&= \frac{e^{-r(T-t)}}{4\pi^2}e^{-\epsilon x(l)'}\sum_{k_1=0}^{N_1}\sum_{k_1=0}^{N_1} e^{\mathrm{i}u(k)x(l)'}\hat{P}(u(k)+\mathrm{i}\epsilon)\Phi(u(k)+\mathrm{i}\epsilon)\\
&= (-1)^{l_1+l_2}e^{-r(T-t)}\left(\frac{\eta N}{4\pi^2}\right)^2 e^{-\epsilon x(l)'} \qquad (2.21)\\
&\quad\cdot\left[\frac{1}{N^2}\sum_{k_1=0}^{N_1}\sum_{k_1=0}^{N_1}(-1)^{k_1+k_2}e^{2\pi\mathrm{i}kl'/N}\hat{P}(u(k)+\mathrm{i}\epsilon)\Phi(u(k)+\mathrm{i}\epsilon)\right]\\
&= (-1)^{l_1+l_2}e^{-r(T-t)}\left(\frac{\eta N}{4\pi^2}\right)^2 e^{-\epsilon x(l)'}\left[\mathsf{ifft2}(H)\right](l),
\end{aligned}$$

where

$$H(k)=(-1)^{k_1+k_2}\hat{P}(u(k)+\mathrm{i}\epsilon)\Phi(u(k)+\mathrm{i}\epsilon),$$

and (again) the third equality 3 in (2.21) holds because of the Nyquist criterion. Set $k=(k_1,k_2), l=(l_1,l_2)$ and $\epsilon=(\epsilon_1,\epsilon_2)$, denote by v' the transpose of the vector v. Abbreviate by *ifft2* the two-dimensional inverse Fourier transform (e.g. as implemented in the epynomous MATLAB function). The the FFT option pricing method can be summarised as in Algorithm 1.

3 Pricing models

Since the focus is to price spread options using the Fourier transform method, we consider pricing models in terms of the characteristic functions of the underlying log asset price distributions.

In our application examples we will consider the four models listed in Table 1:

(a) GBM denotes a two–factor geometric Brownian motion model of asset prices with

$$e = [1, 1],\ \Sigma = \begin{pmatrix} \sigma_1^2 & \sigma_1\sigma_2\rho \\ \sigma_1\sigma_2\rho & \sigma_2^2 \end{pmatrix},\ \text{and } \sigma^2 = \text{diag}(\Sigma).$$

(b) SV denotes the GBM model extended by a third, stochastic volatility factor as in Dempster and Hong (2002), with

$$\begin{cases} \Gamma := \left[2\log\left(\frac{2\theta-(\theta-\gamma)(1-e^{-\theta T})}{2\theta}\right) + (\theta-\gamma)T\right] \\ \zeta := -\frac{1}{2}\left[(\sigma_1^2u_1^2 + \sigma_2^2u_2^2 + 2\rho\sigma_1\sigma_2u_1u_2) + \mathrm{i}(\sigma_1^2u_1 + \sigma_2^2u_2)\right] \\ \gamma := \kappa - \mathrm{i}(\rho_1\sigma_1u_1 + \rho_2\sigma_2u_2)\sigma_\nu \\ \theta := \sqrt{\gamma^2 - 2\sigma_\nu^2\zeta} \end{cases}$$

(c) VG denotes a variance gamma model. This form of a characteristic function is a special case of the one given in Hurd and Zhou (2010), where $\alpha = 1$. By $'$, we mean a transpose of a vector, and Σ is defined as in the GBM case.

(d) NIG denotes a normal inverse Gaussian model along the lines of Eberlein et al. (2010), who apply this model to price options on the minimum/maximum. The structural matrix Δ is assumed to be a positive semidefinite symmetric matrix with unity determinant $\text{Det}(\Delta) = 1$. This matrix is decisive in controlling the degree of correlations between the components of asset price processes. In our case we consider an identity matrix, see also the paper by Eberlein et al. (2010).

4 Spread options in equity market

4.1 Numerical results

This section provides numerical results for all the models under consideration. To take a full advantage of computational speed, all numerical experiments are coded in C++. All code was run on a Dell *Intel(R) Core(TM) i5 - 3.30GHz and with 16 GB memory*. To compute the double discrete Fourier transform, we used the FFTW library (see Frigo and Johnson (2010)). Compared to Matlab, to use two–dimensional inverse FFT in the FFTW library (the *FFTW-backward* method) in C++ is non-trivial. We found that in order to obtain results consistent with the Matlab *ifft2* function using FFTW, one has to scale the FFTW output by the size of the grid, a feature which is not mentioned in the FFTW documentation (e.g. Frigo and Johnson (2010)).

The standard FFT procedures for option pricing of Carr and Madan (1999) involve

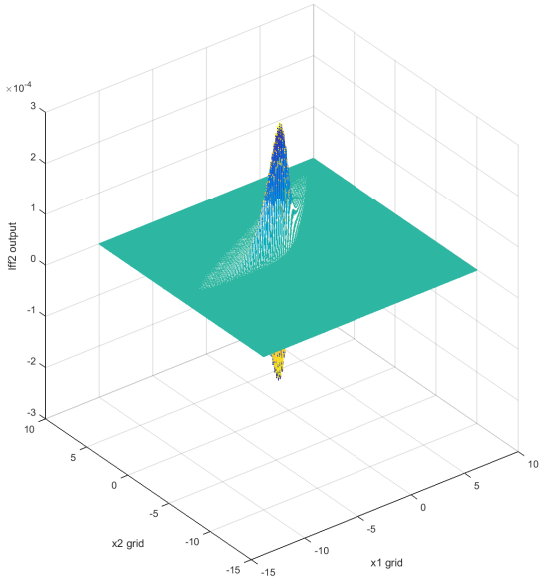

(a) ifft2: Matlab function

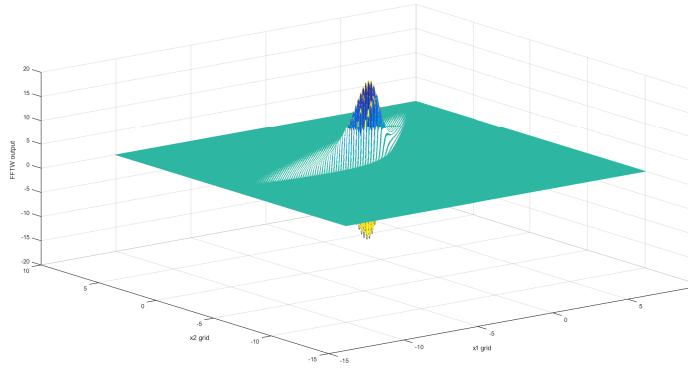

(b) FFTW library (backward): C++

Figure 1: FFT coefficients output comparison

a negative exponent, i.e. $e^{-\mathrm{i}\frac{2\pi}{N}ij}$, and hence one would use FFTW-forward. However, in the Hurd and Zhou (2010) set-up there is a positive sign in the exponent $e^{2\pi \mathrm{i}kl'/N}$ and this implies the use of FFTW-backward. As depicted in Figure 1, to reconcile these differences, we point out here that the output of FFTW backward must always be scaled in order to get the same output as for Matlab built-in function *ifft2*.

Below, we show a snapshot of how to set up two-dimensional FFT using the FFTW library:

```
% MATLAB
% We use the notations as defined above
% Phi represents the joint characteristic function
% P_hat represents the Fourier transform of the payoff function
    ↪ in terms of the complex Gamma function

H=zeros(N,N);
C=zeros(N,N);
for i=0:N-1
    for j=0:N-1
    H(i+1,j+1)=(-1)^(i+j)*Phi([u1(i)+1i*e1 u2(j)+1i*e2 ])*P_hat
        ↪ ([u1(i)+1i*e1 u2(j)+1i*e2 ]);
    C(i+1,j+1)=(-1)^(i+j)*exp(-e1*x1(i+1)-e2*x2(j+1))*((eta*N
```

```
        ↪ /(2*pi))^2);
    end
end
V=real(C.*ifft2(H)); % Price Matrix
```

```
// In C++
fftw_complex  *out, *in;
fftw_plan p; //Variable to store FFT Plan

//Allocate memory for FFT variables; the input and output
   ↪ arrays
        in = (fftw_complex*)fftw_malloc(sizeof(fftw_complex)*
           ↪ nd); //where nd:=N x N
        out = (fftw_complex*)fftw_malloc(sizeof(fftw_complex)*
           ↪ nd);

    //creating a plan: i.e ifft2
        p = fftw_plan_dft_2d(N, N, in, out, FFTW_BACKWARD,
           ↪ FFTW_MEASURE);

    //computing the actual transforms
        fftw_execute(p); // ifft2 out[i][j]

vector<double> V(nd);// Vector containing prices
vector<double> C(nd);//
   for (int i = 0; i < N; i++){
        for (int j = 0; j < N; j++){
            C[i*N + j] = pow(-1, i + j)*pow((eta*N / (2 * pi)),
               ↪  2)*exp(-e1*x1[i] - e2*x2[j]);
                V[i*N + j] = C[i*N +j]* out[i*N + j][0]/nd; //
                   ↪ Note: the scaling here by nd
                }
        }
```

4.1.1 Model parameters

All our results for FFT performance are benchmarked against Monte Carlo with 10000000 simulations using 1000 time steps, and we also provide the 95% level Monte Carlo con-

Table 3: GBM parameters: $\sigma_1 = 0.2, \sigma_2 = 0.1, \rho = 0.5$

Strike K	**Hurd/Zhou result**	**Kirk approx**	**FFT**	**Monte Carlo**		
				Value	**95% conf. level**	
0.4	8.312461	8.30085	8.31318	8.31356	8.29359	8.34012
0.8	8.114994	8.09336	8.11577	8.10179	8.10327	8.14941
1.2	7.92082	7.88952	7.92158	7.91399	7.90194	7.94758
1.6	7.729932	7.68933	7.7308	7.73813	7.72171	7.76697
2	7.542324	7.49278	7.54315	7.55118	7.55824	7.60309
2.4	7.357984	7.29986	7.35878	7.34552	7.32802	7.37229
2.8	7.176902	7.11055	7.1777	7.17983	7.16752	7.21136
3.2	6.999065	6.92485	6.99984	6.99551	6.97241	7.701575
3.6	6.824458	6.74273	6.82531	6.81754	6.81667	6.85962
4	6.653065	6.56417	6.65374	6.64457	6.61088	6.65325

fidence interval for the spread option value $\mathbb{V}$ given by:

$$\left(\mathbb{V} - z_{1-\frac{\alpha}{2}}\frac{s}{\sqrt{N}}, \mathbb{V} + z_{1-\frac{\alpha}{2}}\frac{s}{\sqrt{N}}\right),$$

where the quantity $\frac{s}{\sqrt{N}}$ is the *standard error* of the Monte Carlo estimate and $z_{1-\frac{\alpha}{2}}$ is the quantile from the standard normal distribution corresponding to a (two–sided) confidence level of α. Additionally, in the case of GBM, SV and VG, we also quote as a benchmark prices given in Hurd and Zhou (2010).

Table 2 shows the parameters common to all models and these inputs are taken from Hurd and Zhou (2010) paper where d_1 and d_2 represent the dividend rate for S_1 and S_2 respectively.

Table 2: Common inputs to all models

S_1	S_2	r	T	d_1	d_2
100	96	0.1	1.0	0.05	0.05

4.1.2 GBM model

Table 3 shows the results for GBM model with additional inputs ρ, σ_1 and σ_2 and again these inputs are taken from Hurd and Zhou (2010). As can be seen from this table, the FFT result lies within the Monte Carlo confidence bounds, unlike Kirk's approximation.

4.1.3 3-Stochastic volatility model

The results for SV model are presented in Table 4. Again, our results are consistent with Hurd and Zhou (2010) and lie within the Monte Carlo confidence bounds.

Table 4: SV results: $\sigma_1 = 1.0, \sigma_2 = 0.5, \sigma_\nu = 0.05, \nu_0 = 0.04$
$\kappa = 1.0, \mu = 0.04, \rho = 0.5, \rho_1 = -0.5, \rho_2 = 0.25$

Strike K	**Hurd/Zhou result**	**FFT**	**Monte Carlo**		
			value	**95% conf. level**	
2	7.548502	7.54934	7.52391	7.51777	7.56067
2.2	7.453536	7.45438	7.50048	7.42498	7.46758
2.4	7.359381	7.36014	7.32819	7.36815	7.41071
2.6	7.266037	7.26679	7.21304	7.2505	7.29275
2.8	7.173501	7.1743	7.20518	7.1452	7.18715
3	7.081775	7.08266	7.12544	7.07343	7.11519
3.2	6.990857	6.99168	7.03087	6.95522	6.99667
3.4	6.900745	6.90135	6.90931	6.88184	6.92307
3.6	6.81144	6.81218	6.81998	6.78234	6.82333
3.8	6.722939	6.72382	6.74597	6.71553	6.75641

Table 5: VG results: $\theta_1 = -0.6094, \theta_2 = -0.8301, \sigma_1 = 0.0325$
$\sigma_2 = 0.9406, \nu = 0.2570, \rho = 0.5$

Strike K	**FFT**	**Monte Carlo**		
		value	**95% conf. level**	
2	31.2167	31.2252	31.1693	31.281
2.2	31.0922	31.0913	31.0355	31.147
2.4	30.9677	30.9803	30.9247	31.0359
2.6	30.8435	30.8894	30.8339	30.9449
2.8	30.7194	30.7165	30.6612	30.7718
3	30.5954	30.6253	30.57	30.6806
3.2	30.4716	30.4617	30.4066	30.5168
3.4	30.348	30.259	30.2041	30.314
3.6	30.2245	30.2296	30.1747	30.2845
3.8	30.1011	30.0902	30.0355	30.1449

4.1.4 Variance Gamma model

In Tables 5 and 6, we show the result under VG model. Table 5 show the results for the special case of a 2-dimensional Variance Gamma model given in Hurd and Zhou (2010) (as before we set $\alpha = 1$ to allow maximum dependence between the two asset return, keeping their distribution unchanged). We run a Monte Carlo simulation and to compare FFT prices. These parameters are taken from Chapter 4, p.190 of the book by Kienitz and Wetterau (2012). While in Table 6, we considered VG characteristic representation given in the study paper and compare FFT values to the given benchmark values.

Table 6: VG result2: $a_p = 20.4499, a_n = 24.4499, \alpha = 0.4, \lambda = 10$

Strike K	FFT	Benchmark	Error
2	9.72793	9.727458	-4.72E-04
2.2	9.63048	9.630005	-4.75E-04
2.4	9.53366	9.533199	-4.61E-04
2.6	9.43751	9.43704	-4.70E-04
2.8	9.34199	9.341527	-4.63E-04
3	9.24714	9.246662	-4.78E-04
3.2	9.1529	9.152445	-4.55E-04
3.4	9.05929	9.058875	-4.15E-04
3.6	8.96646	8.965954	-5.06E-04
3.8	8.87415	8.873681	-4.69E-04
4	8.78246	8.782057	-4.03E-04

4.1.5 Normal inverse Gaussian model

The result for NIG models are given in Table 7. We chose a symmetric centered NIG ($\mu_1 = 0, \mu_2 = 0$ and $\Delta =$ **I**). Figure 2 plots the deviation of the FFT price outside the 95% confidence interval of Monte Carlo prices. Deviations outside the Monte Carlo confidence bounds are within what could be expected due to random variation. As a benchmark (labelled "Integration") we have used the method of Caldana and Fusai (2013) in this case.

Table 7: NIG results: $\mu_1 = 0, \mu_2 = 0, \alpha = 6.20, \delta = 0.150$
$\beta_1 = -3.80, \beta_2 = -2.50, \rho = 0$

Strike K	FFT	Integration	Monte Carlo		
			value	95% conf. level	
2	9.49266	9.49119	9.48459	9.45828	9.51052
2.2	9.38858	9.38720	9.403	9.37675	9.42925
2.4	9.28489	9.28392	9.28919	9.26305	9.31533
2.6	9.18231	9.18136	9.18328	9.15721	9.20935
2.8	9.08077	9.07952	9.07361	9.0477	9.09952
3	8.98013	8.97840	8.99533	8.96951	9.02116
3.2	8.87969	8.87800	8.87543	8.84968	8.90118
3.4	8.77912	8.77834	8.77178	8.74624	8.79733
3.6	8.68022	8.67940	8.67697	8.65143	8.70251
3.8	8.58309	8.58119	8.55386	8.52848	8.57925

The overall results for all models are presented in Table 8. SSE is calculated by summing the square errors for 10 options with benchmark values.

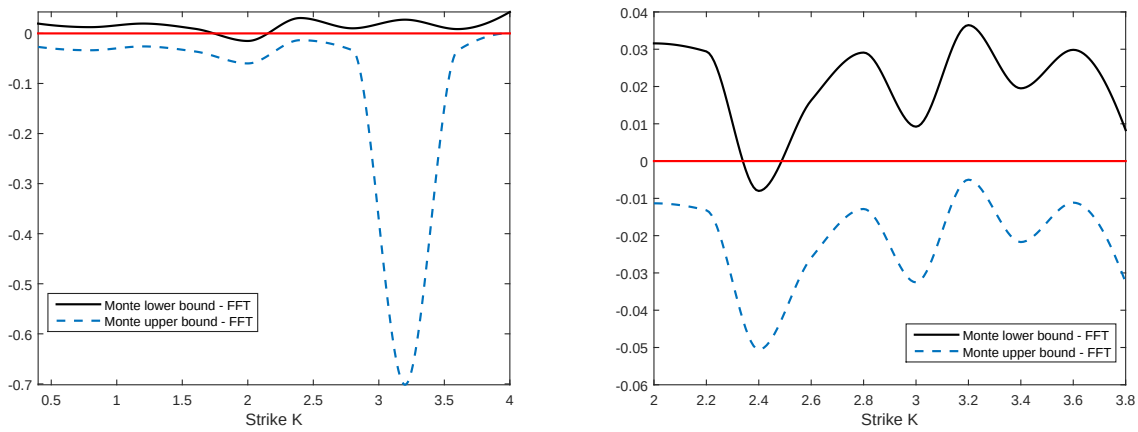

(a) GBM model

(b) NIG model

Figure 2: FFT prices deviation from the 95% level Monte Carlo confidence interval.

Table 8: Summary for models results

Overall results	FFT		Monte Carlo	
	$\bar{u}$	Grid size (N)	Simulation	Time steps
	40	256	1000000	250

Method\Model	GBM	SV	VG	NIG
FFT Time (s)	0.001	0.002	0.001	0.001
Monte Carlo Time (s)	254.392	390.006	445.113	443.162

4.2 The effect of N, $\overline{u}$ and (ϵ_1, ϵ_2)

The main advantage of FFT is that one obtains a sufficiently good numerical price approximation within minimum time. In the following, we analyse the sensitivity due to the truncation and discretization parameters under the NIG model (all other models under consideration were analysed in this respect by Hurd and Zhou (2010)). Again, we compute 10 options with different strike prices and then we calculate the sum of the squared errors. Note that Hurd and Zhou varies assets prices processes S_1 and S_2 in this analysis because $K = 1$, in our case, we fixed all parameters given above, and considered $K = 40 - i,\ i = 0, \cdots 9$. To get the benchmark values, we run 10000000 Monte Carlo simulations with 1000 time steps. Results are presented in Table 9 and in Figure 3. Already, with a tight integration range, we get a sufficiently small error even with relatively small N. Figure 3 shows the effect of changing integration truncation width and the number of grid points. Increasing N narrows the grid spacing thereby lowering the truncation error, while a larger integration range $[-\overline{u}, \overline{u}]$ results in truncation difficulties and hence pure discretization errors (marked red) increase.

Table 9: Sum of the squared errors for 10 Spread options under NIG model by changing N and $\overline{u}$

N\$\overline{u}$	**20**	**40**	**60**	**80**	**100**	**160**
64	0.000863	0.217084	6.780534	39.9114		
128	0.001038	0.000105	0.00603	0.217393		
256	0.001037	0.00017	0.000159	9.84E-05	0.000167	0.217411999
512	0.001037	0.00017	0.000162	0.000161	0.00016	9.79934E-05
1024	0.001037	0.00017	0.000162	0.000161	0.00016	0.000159978
2048	0.001037	0.00017	0.000162	0.000161	0.00016	0.000159981

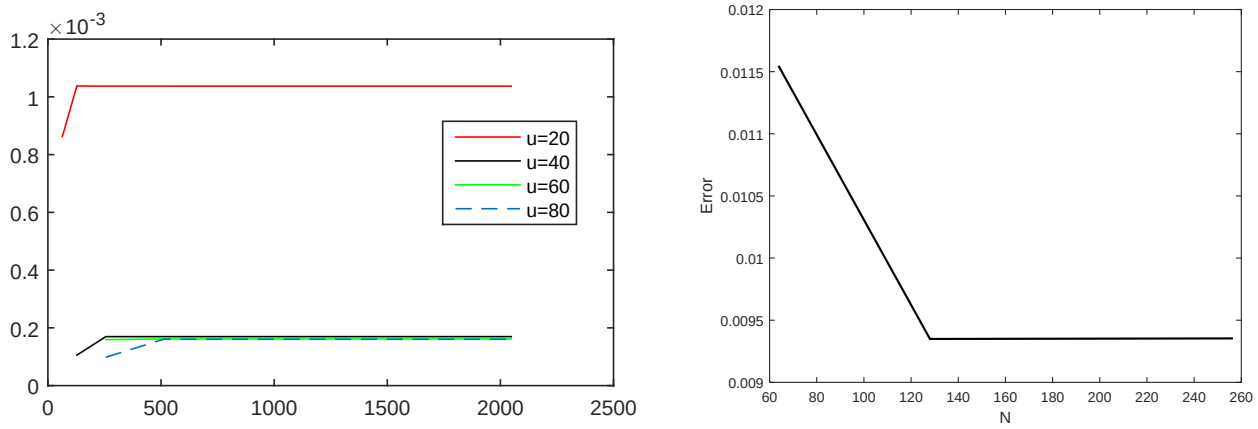

Figure 3: FFT errors for NIG as $\overline{u}$ and N are varied.

Table 10 and Figure 4 show the model sensitivity to the choice of ϵ_1 and ϵ_2 which serves to provide the degree of integrability. As noted by Hurd and Zhou (2010), GBM and SV model are not very sensitive to the choices of the damping parameters. VG model is however sensitive to ϵ_1 and ϵ_2, and hence these must be chosen carefully.

In the NIG model, one can observe that although $\epsilon_2 > 0$ and $\epsilon_1 + \epsilon_2 < -1$ we still have higher truncation error in case when $\epsilon_2 = 0.2$. In this case, NIG is only sensitive to ϵ_2. With our initial choice of $(-3, 1)$, we obtain reasonable results.

Table 10: NIG model: sum of the squared error, computed for 10 options by changing damping parameters ϵ_1 and ϵ_2.

$\epsilon_2\backslash\epsilon_1$	**-4.4**	**-4.2**	**-4**	**-3.8**	**-3.6**	**-3.4**	**-3.2**	**-3**
0.2	2.808423	2.79587	2.789595	2.786387	2.784967	2.784178	2.783868	2.783596
0.4	0.001169	0.001161	0.001158	0.001156	0.001155	0.001154	0.001154	0.001154
0.6	0.000154	0.000154	0.000154	0.000154	0.000154	0.000154	0.000154	0.000154
0.8	0.000151	0.000151	0.000151	0.000151	0.000151	0.000151	0.000151	0.000151
1	0.000151	0.000151	0.000151	0.000151	0.000151	0.000151	0.000151	0.000151
1.2	0.000151	0.000151	0.000151	0.000151	0.000151	0.000151	0.000151	0.000151
1.4	0.000151	0.000151	0.000151	0.000151	0.000151	0.000151	0.000151	0.000151
1.6	0.000151	0.000151	0.000151	0.000151	0.000151	0.000151	0.000151	0.000179

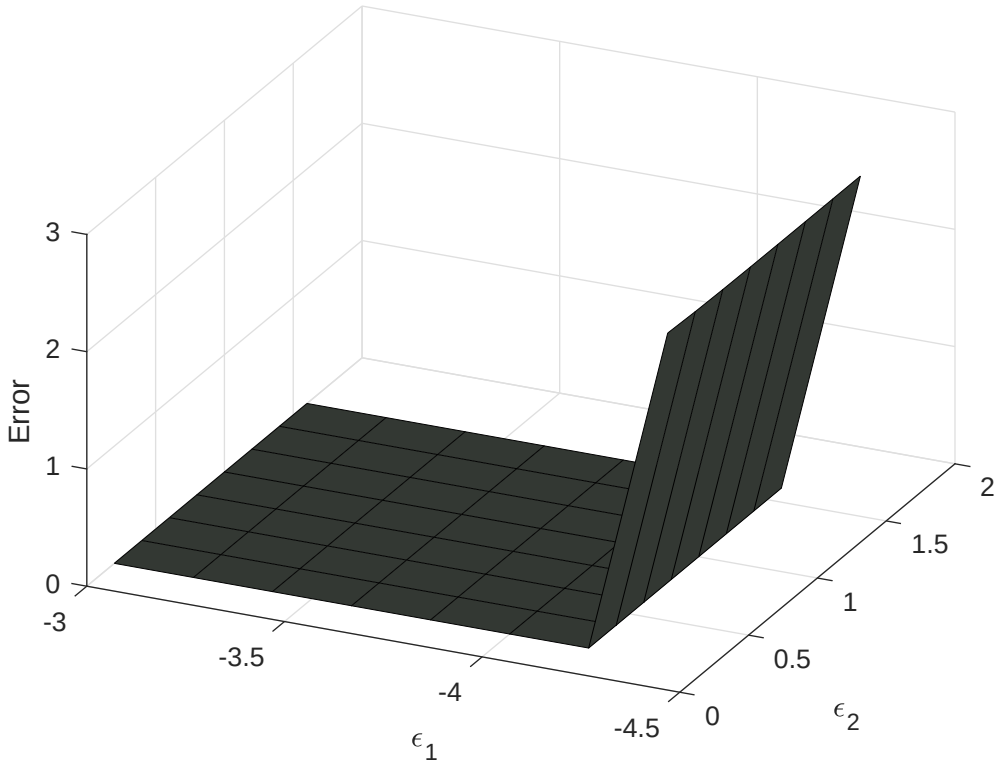

Figure 4: FFT errors for NIG model: Sensitivity to damping parameters (ϵ_1, ϵ_2), where the error is the sum of the square errors on ten options and it is calculated by Error $= \frac{1}{10}\sum_{i=0,j=0}^{9}\left[(\text{FFT price}_{ij} - \text{Monte Carlo price}_{ij})^2\right]$

4.3 Volatility sensitivity

Volatility is one of the important model parameters and therefore we proceed to illustrate its impact on prices calculated using the FFT approach in the GBM and VG models. We also compute the derivative with respect to these parameters, i.e. *vega*.

Figure 5 shows the change is spread option value with respect to the change in σ_1 and σ_2. In the GBM model, lower values of σ_1 (keeping σ_2 fixed) give lower values for the option premium. In VG model, the result is counterintuitive, σ_1 does not seems to play a big role here. Keeping σ_2 fixed, and varying σ_1 results in a smile–like shape.

Formally, the sensitivity with respect to sigma parameter is given by:

$$\frac{\partial \mathbb{V}}{\partial \sigma_-} = (-1)^{l_1+l_2} e^{-r(T-t)} \left(\frac{\eta N}{4\pi^2}\right)^2 e^{-\epsilon x(l)'} \left[\text{ifft2}\left(\frac{\partial H}{\partial \sigma_-}\right)\right](l),$$

where $\frac{\partial}{\partial \sigma_-}$ means a partial derivative with respect to either σ_1 or σ_2.

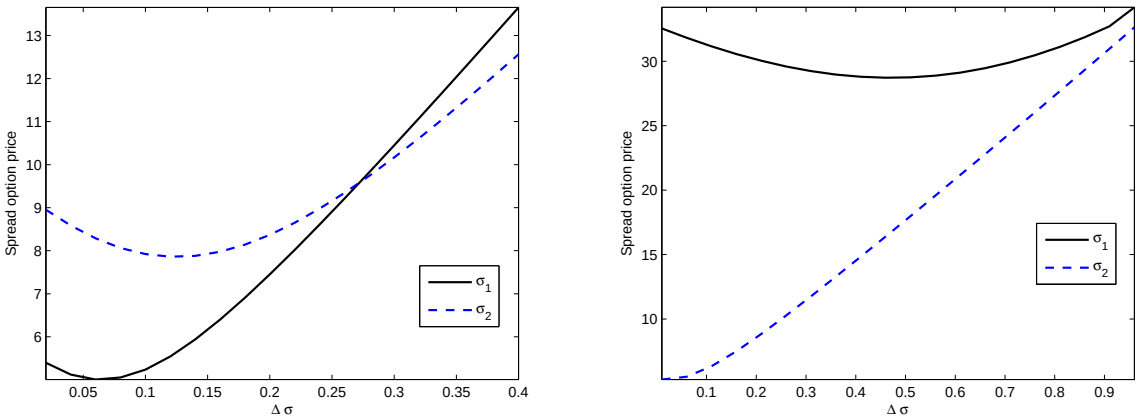

(a) The GBM model (b) The VG model

Figure 5: Spread option price sensitivity to the change in σ_1 and σ_2

In the GBM case,

$$\begin{aligned}\frac{\partial H}{\partial \sigma_-} &= (-1)^{k_1+k_2}\hat{P}(u(k)+\mathrm{i}\epsilon)\frac{\partial}{\partial \sigma_-}\Phi(u(k)+\mathrm{i}\epsilon)\\ &= \left(-\frac{T}{2}\mathrm{i}(u(k)+\mathrm{i}\epsilon)\frac{\partial}{\partial \sigma_-}\sigma^2 - \frac{T}{2}(u(k)+\mathrm{i}\epsilon)\frac{\partial \Sigma}{\partial \sigma_-}(u(k)+\mathrm{i}\epsilon)'\right)\\ &\quad \cdot (-1)^{k_1+k_2}\hat{P}(u(k)+\mathrm{i}\epsilon)\Phi(u(k)+\mathrm{i}\epsilon)\\ &= -\frac{T}{2}(u(k)+\mathrm{i}\epsilon)\left(\mathrm{i}\frac{\partial \sigma^2}{\partial \sigma_-} + \frac{\partial \Sigma}{\partial \sigma_-}(u(k)+\mathrm{i}\epsilon)'\right)H(l).\end{aligned} \tag{4.1}$$

In the VG model case, notice that the risk-neutral characteristic function is given by (see also Luciano and Schoutens (2006)),

$$\Phi(u_1,u_2) = \exp\left(\mathrm{i}u_1 m_1 T + \mathrm{i}m_2 T\right)\left(1 - iu_1\theta_1\nu - iu_2\theta_2\nu + \nu u'\Sigma u/2\right)^{-\frac{T}{\nu}},$$

where

$$m_1 = r - d_1 + W_1 \text{ and } m_2 = r - d_2 + W_2,$$

and the martingale corrections are given by

$$W_1 = \log(1-\theta_1\nu - \frac{1}{2}\sigma_1^2\nu)/\nu \text{ and } W_2 = \log(1-\theta_2\nu - \frac{1}{2}\sigma_2^2\nu)/\nu.$$

As seen from GBM calculation for $\frac{\partial \mathbb{V}}{\partial \sigma_-}$, we simply have to find $\frac{\partial \Phi}{\partial \sigma_-}$. For example, the partial derivative with respect to σ_1 is given by the product rule of differentiation:

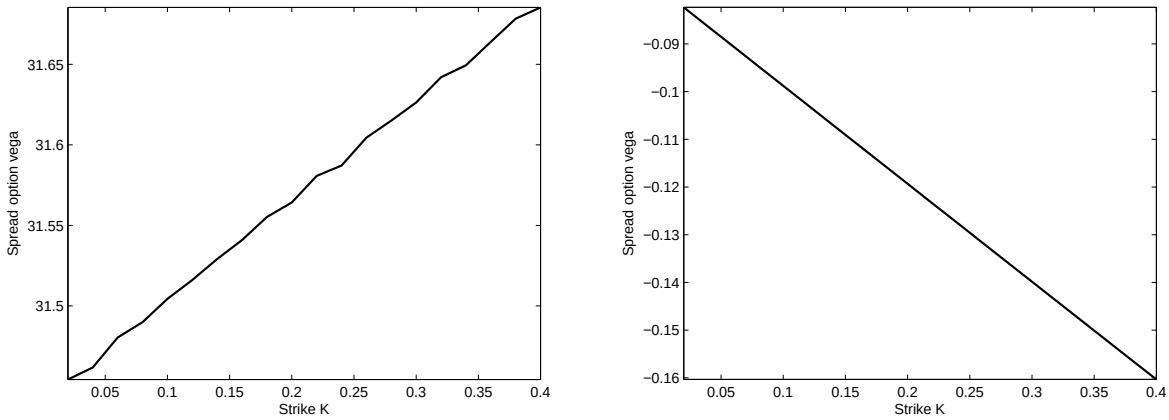

(a) vega for σ_1 (b) vega for σ_2

Figure 6: vega under the GBM model

$$\begin{aligned}\frac{\partial \Phi}{\partial \sigma_1} &= \mathrm{i}u_1 T \frac{\partial m_1}{\partial \sigma_1} \exp\left(\mathrm{i}u_1 m_1 T + \mathrm{i}m_2 T\right)\left(1 - iu_1\theta_1\nu - iu_2\theta_2\nu + \nu u'\Sigma u/2\right)^{-\frac{T}{\nu}} \\ &+ \left(-\frac{T}{\nu}\right) \exp\left(\mathrm{i}u_1 m_1 T + \mathrm{i}m_2 T\right)\left(1 - iu_1\theta_1\nu - iu_2\theta_2\nu + \nu u'\Sigma u/2\right)^{-\frac{T}{\nu}-1} \\ &\times \frac{\nu}{2} u' \frac{\partial \Sigma}{\partial \sigma_1} u.\end{aligned} \tag{4.2}$$

Note, where u is not specified, it means a vector consisting of u_1 and u_2. Finally, vega calculation for VG model is then straight forward by letting $u_1 = u_1 + \mathrm{i}\epsilon_1$, $u_2 = u_2 + \mathrm{i}\epsilon_2$ and also note that

$$\frac{\partial \Sigma}{\partial \sigma_1} = \begin{pmatrix} 2\sigma_1 & \sigma_2\rho \\ \sigma_2\rho & 0 \end{pmatrix}, \text{ and } \frac{\partial \sigma^2}{\partial \sigma_1} = \begin{pmatrix} 2\sigma_1 \\ 0 \end{pmatrix}.$$

Figures 6 and 7 show the plot for vegas across different strikes for GBM and VG mode respectively. GBM has higher vega for σ_1 (as expected from Figure 5) while VG has higher vegas for σ_2.

5 Spread options in the fixed-income markets

In this section, we apply Hurd and Zhou (2010) apparatus to spread options in fixed income markets. We compare our results to the lower bound formula for spread options by Caldana and Fusai (2013).

We consider two examples. The first one is pricing a spread option on two LIBORs based on different currencies, domestic and foreign currency. In the second example we consider LIBOR formula in the presence of roll–over risk developed in Alfeus et al.

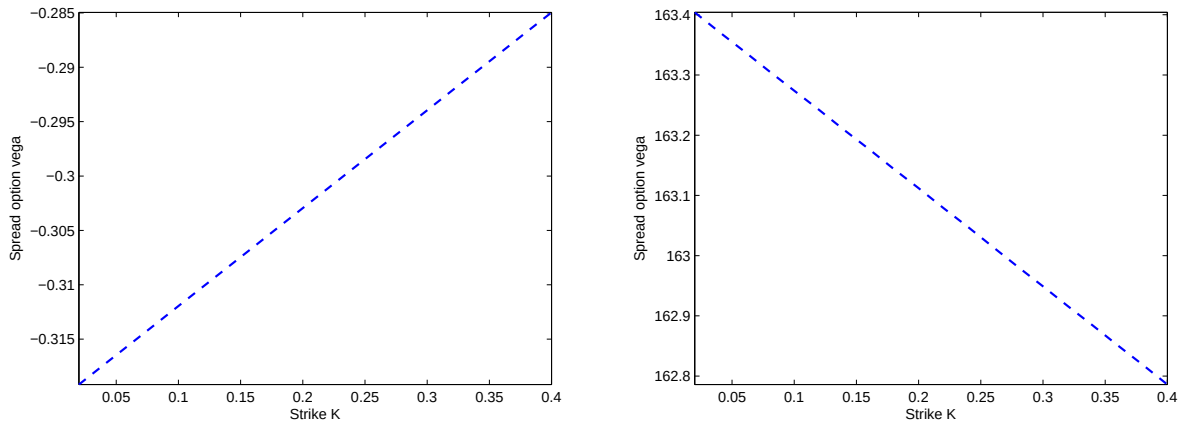

(a) vega for σ_1

(b) vega for σ_2

Figure 7: vega under the VG model

(2017) and explore the case where the LIBOR–OIS spread is driven solely by renewal risk,[6] proceeding to price an option on this spread.

5.1 Currency spread options

Here we consider a spread option on two LIBORs in different currencies using the two-dimensional FFT pricing method, under a multicurrency lognormal LIBOR Market Model along the lines of Schlögl (2002). We follow the notation of Brigo and Mercurio (2006) (see p. 633–637 therein). Brigo and Mercurio (2006) also provide an approximate analytical formula for this option (see also Mercurio (2002)), which we will use as a comparison.

Assume that we are given a domestic market and a foreign market. Suppose that the term structures of discount factors that are observed in the domestic and foreign markets at time t are respectively given by $T \mapsto P(t,T)$ and $T \mapsto P^f(t,T)$ for $T \geq t$, where $P(t,T)$ is the price at time t of a zero coupon bond maturing at time T. Consider the future times T_{i-1} and T_i, $i = 1, \cdots, N$. The domestic and foreign forward rates at time t for the interval $[T_{i-1}, T_i]$ are, respectively,

$$\begin{aligned} F_i(t) &= F(t; T_{i-1}, T_i) = \frac{P(t,T_{i-1}) - P(t,T_i)}{\delta_i P(t,T_i)}, \\ F_i^f(t) &= F^f(t; T_{i-1}, T_i) = \frac{P^f(t,T_{i-1}) - P^f(t,T_i)}{\delta_i P^f(t,T_i)}. \end{aligned} \tag{5.1}$$

[6] the influence of funding liquidity component set to zero.

Table 11: Parameters

T	$D(t,T)$	$D(t,T)^f$	σ	σ^f	$F(t)$	$F(t)^f$	K
0.25	0.9978	0.9877	0.125	0.137			
0.5	0.9896	0.9812	0.13	0.13	0.033145	0.026498	0.006647
0.75	0.9814	0.9747	0.135	0.125	0.033422	0.026675	0.006747
1	0.9732	0.9682	0.14	0.13	0.033703	0.026854	0.006849
1.25	0.965	0.9617	0.145	0.142	0.03399	0.027035	0.006954
1.5	0.9568	0.9552	0.15	0.145	0.034281	0.027219	0.007062
1.75	0.9486	0.9487	0.155	0.123	0.034577	0.027406	0.007171
2	0.9404	0.9422	0.16	0.14	0.034879	0.027595	0.007284
2.25	0.9322	0.9357	0.165	0.145	0.035186	0.027787	0.007399
2.5	0.924	0.9292	0.17	0.148	0.035498	0.027981	0.007517
2.75	0.9158	0.9227	0.175	0.156	0.035816	0.028178	0.007638
3	0.9076	0.9162	0.18	0.162	0.036139	0.028378	0.007761

Denoting by $F_X(t,T_i)$ the forward exchange rate at time t for maturity T_i,

$$F_X(t,T_i) = X(t)\frac{P^f(t,T_i)}{P(t,T_i)},$$

where $X(t)$ is the spot exchange rate. Assuming constant volatilities, the two forward rates evolves under the domestic forward measure $\mathbb{Q}^i$ according to

$$\begin{aligned} dF_i(t) &= \sigma_i F_i(t) dW_i(t), \\ dF_i^f(t) &= F_i^f(t)[-\rho\sigma_{FX}\sigma_i^f dt + \sigma_i^f dW_i^f(t)], \end{aligned} \tag{5.2}$$

where

$$d[W_i, W_i^f] = \rho dt.$$

The forward exchange rate dynamics of $F_X(t,T_i)$ are given by

$$dF_X(t,T_i) = \sigma_{FX} F_X(t,T_i) dW_X(t),$$

where the forward exchange rate volatility σ_{FX} is taken as a constant.

Now, consider a spread option on the two LIBOR rates $L(T_{i-1},T_i)$ and $L^f(T_{i-1},T_i)$ with a payoff (in domestic currency)

$$\delta_i \left(L^f(T_{i-1},T_i) - L(T_{i-1},T_i) - K\right)^+,$$

Table 12: Spread option prices, $\sigma_{FX} = 0.225$.

					Monte carlo		
K	**HZ FFT**	**Approx.**[7]	**Integration**	**Rel Error**	**Low Bound**	**Price**	**Upper bound**
0.006647	0.000186	0.00017864	0.000178632	0.039556	0.0001786	0.000179	0.000178912
0.006747	0.000266	0.000264108	0.000264088	0.00779	0.0002640918	0.0002641	0.000264478
0.006849	0.000338	0.000337485	0.000337453	0.002164	0.000337392	0.000338	0.000337984
0.006954	0.000413	0.000412378	0.000412321	0.000706	0.000412303	0.000413	0.000413026
0.007062	0.000493	0.000492884	0.000492777	0.00034	0.000492806	0.000493	0.000493662
0.007171	0.000565	0.000564559	0.000564409	0.000279	0.000564385	0.000565	0.000565369
0.007284	0.00061	0.000610265	0.000610164	0.000173	0.0006102	0.000611	0.000611317
0.007399	0.000693	0.000693254	0.000693051	0.000321	0.000693697	0.000694	0.000694321
0.007517	0.000766	0.000766459	0.000766186	0.000399	0.000766242	0.000767	0.00076763
0.007638	0.000838	0.000837814	0.000837472	0.000452	0.00083768	0.000838	0.000839213
0.007761	0.000917	0.000917185	0.000916709	0.000558	0.000916944	0.000918	0.000918623

and the no-arbitrage value at time t of the above payoff is given by

$$\begin{aligned}\mathcal{S}_t &= \delta_i P(t,T_i)\mathbb{E}^{\mathbb{Q}^i}\left[\left(L^f(T_{i-1},T_i) - L(T_{i-1},T_i) - K\right)^+\right] \\ &= \delta_i P(t,T_i)\mathbb{E}^{\mathbb{Q}^i}\left[\left(F^f(T_{i-1}) - F(T_{i-1}) - K\right)^+\right] \\ &= \delta_i K P(t,T_i)\mathbb{E}^{\mathbb{Q}^i}\left[\left(e^{x^f} - e^x - 1\right)^+\right],\end{aligned} \tag{5.3}$$

where

$$x^f = \log\left(\frac{F_i^f(T_{i-1})}{K}\right), \text{ and } x = \log\left(\frac{F_i(T_{i-1})}{K}\right).$$

We can now apply Hurd and Zhou (2010) where the joint characteristic function of $X_T = \left(\log(L^f(T_{i-1}), \log(L(T_{i-1})\right)$ is of the form $e^{\mathrm{i}uX_0'}\Phi(u;T_i)$ where

$$\Phi(u;T_i) = \exp\left(\mathrm{i}u\left(M_x T - \frac{1}{2}\sigma^2 T\right)' - \frac{1}{2}u\Sigma u' T\right), \tag{5.4}$$

where

$$X_0 = \begin{bmatrix}\log\left(\frac{F_i^f(t)}{K}\right) \\ \log\left(\frac{F_i(t)}{K}\right)\end{bmatrix}, M_x = \begin{bmatrix}-\frac{1}{2}\sigma_i \\ -\rho\sigma_{FX}\sigma_i^f - \frac{1}{2}\sigma_i^f\end{bmatrix}, \Sigma = \begin{pmatrix}\sigma_i^2 & \sigma_i\sigma_i^f\rho \\ \sigma_i\sigma_i^f\rho_i & (\sigma_i^f)^2\end{pmatrix}, \text{ and } \sigma^2 = \text{diag}(\Sigma).$$

Numerical example

As Table 12 shows, except for very short maturities, the FFT method delivers accurate results. For this particular case, however, the approximate analytical solution performs as well or better, especially for short maturities.

[7] "Approx." denotes prices calculated using pseudo-analytical formula (Brigo and Mercurio, 2006, p. 635).

5.2 LIBOR–OIS spread options

Alfeus et al. (2017) explicit take into account the risk incurred when borrowing at a shorter tenor versus lending at a longer tenor ("roll–over risk"), resulting in a frequency basis arising endogenously in the model. Thus, the model is consistent with the LIBOR/OIS spread observed in the market. The roll–over risk consists of two components, a credit risk component due to the possibility of being downgraded and thus facing a higher credit spread when attempting to roll over short–term borrowing, and a component reflecting the (systemic) possibility of being unable to roll over short–term borrowing at the reference rate (e.g., LIBOR) due to an absence of liquidity in the market.

Denote by $\mathbb{Q}$ the risk–neutral measure associated with taking the continuously compounded savings account as the numeraire. If we ignore funding liquidity risk, then in the framework of Alfeus et al. (2017) spot LIBOR observed at time t with maturity T can be expressed as

$$L(t,T) = \frac{1}{\delta}\left(\frac{1}{\mathbb{E}_t^{\mathbb{Q}}\left[e^{-\int_t^T (r_c(s)+\lambda(s)q)ds}\right]} - 1\right) \tag{5.5}$$

where r_c is the continuously compounded short rate abstraction of the interbank overnight rate (e.g., Fed funds rate or EONIA). This is equal to the riskless (default-free) continuously compounded short rate r plus a credit spread. $\lambda(s)q$ is the idiosyncratic credit spread (i.e., of a particular, fixed obligor) over $r_c(s)$, and $\delta = T - t$.

Consider an option on the spread between LIBOR $L(T_{i-1}, T_i)$ and OIS(T_{i-1}, T_i), with the contract strike K. The payoff is given by

$$\delta\left(L(T_{i-1},T_i) - \text{OIS}(T_{i-1},T_i) - K\right)^+ \tag{5.6}$$

where the overnight index swap rate (when $\delta < 1$ year) is given by[8]

$$\text{OIS}(t,T) = \frac{1}{\delta}\left(\frac{1}{\mathbb{E}_t^{\mathbb{Q}}\left[e^{-\int_t^T r_c(s)ds}\right]} - 1\right) \tag{5.7}$$

Assuming that the spread option is collateralised to manage counterparty credit risk, with collateral accruing interest at r_c, the price of (5.6) at time $t \leq T_{i-1}$ can be written as

$$\mathcal{S}_t = \mathbb{E}_t^{\mathbb{Q}}\left[e^{-\int_t^{T_i} r_c(s)ds}\delta\left(L(T_{i-1},T_i) - OIS(T_{j-1},T_j) - K\right)^+\right] \tag{5.8}$$

[8]For details see e.g. Alfeus et al. (2017).

Denote by $D^{\text{OIS}}(t,T)$ the OIS discount factor, i.e.

$$D^{\text{OIS}}(t,T) = \mathbb{E}_t^{\mathbb{Q}}\left[e^{-\int_t^T r_c(s)ds}\right] \tag{5.9}$$

Then, changing to the forward measure $\mathbb{Q}_{T_i}$ with the numeraire $D^{\text{OIS}}(t,T_i)$,

$$\begin{aligned}
\mathcal{S}_t =& D^{\text{OIS}}(t,T_i)\mathbb{E}_t^{\mathbb{Q}_{T_i}}\left[\delta\left(L(T_{i-1},T_i) - OIS(T_{i-1},T_i) - K\right)^+\right] \\
=& D^{\text{OIS}}(t,T_i)\mathbb{E}_t^{\mathbb{Q}_{T_i}}\left[\left(\frac{1}{\mathbb{E}_{T_{i-1}}^{\mathbb{Q}}\left[e^{-\int_{T_{i-1}}^{T_i}(r_c(s)+\lambda(s)q)ds}\right]} - \frac{1}{\mathbb{E}_{T_{i-1}}^{\mathbb{Q}}\left[e^{-\int_{T_{i-1}}^{T_i}(r_c(s)ds}\right]} - \delta K\right)^+\right] \\
=& D^{\text{OIS}}(t,T_i)\delta K\mathbb{E}_t^{\mathbb{Q}_{T_i}}\left[\left(\frac{1}{\delta K}\frac{1}{\mathbb{E}_{T_{i-1}}^{\mathbb{Q}}\left[e^{-\int_{T_{i-1}}^{T_i}(r_c(s)+\lambda(s)q)ds}\right]} - \frac{1}{\delta K}\frac{1}{\mathbb{E}_{T_{i-1}}^{\mathbb{Q}}\left[e^{-\int_{T_{i-1}}^{T_i}(r_c(s)ds}\right]} - 1\right)^+\right] \\
=& D^{\text{OIS}}(t,T_i)\delta K\mathbb{E}_t^{\mathbb{Q}_{T_i}}\left[\left(e^{X_1(T_{i-1})} - e^{X_2(T_{i-1})} - 1\right)^+\right],
\end{aligned} \tag{5.10}$$

where

$$e^{X_1(T_{i-1})} = \frac{1}{\delta K}\frac{1}{\mathbb{E}_{T_{i-1}}^{\mathbb{Q}}\left[e^{-\int_{T_{i-1}}^{T_i}(r_c(s)+\lambda(s)q)ds}\right]}. \tag{5.11}$$

$$e^{X_2(T_{i-1})} = \frac{1}{\delta K}\frac{1}{\mathbb{E}_{T_{i-1}}^{\mathbb{Q}}\left[e^{-\int_{T_{i-1}}^{T_i}(r_c(s)ds}\right]}. \tag{5.12}$$

As in Alfeus et al. (2017), we assume that the model is driven by d independent factors y_i, i.e.

$$r_c(t) = a_0(t) + \sum_{i=1}^{d} a_i y_i(t) \tag{5.13}$$

$$\lambda(t) = b_0(t) + \sum_{i=1}^{d} b_i y_i(t) \tag{5.14}$$

$$\tag{5.15}$$

where the y_i follow Cox–Ingersoll–Ross (CIR) dynamics[9] under the pricing measure, i.e.

$$dy_i(t) = \kappa_i(\theta_i - y_i(t))dt + \sigma_i\sqrt{y_i(t)}dW_i(t), \tag{5.16}$$

[9]These dynamics were first introduced into interest rate term structure modelling by Cox et al. (1985).

where $dW_i(t) \quad (i = 1, \cdots, d)$ are independent Wiener processes.

We can now write

$$\begin{aligned} e^{X_1(T_{i-1})} =& \frac{1}{\delta K} \frac{1}{e^{-\int_{T_{i-1}}^{T_j}(a_0(s)+b_0(s)q)ds+\sum_{n=1}^{d}(\Phi_n(T_{i-1},T_i,a_n+b_nq,0)+y_n(T_{i-1})\Psi_n(T_{i-1},T_i,a_n+b_nq,0))}} \\ =& \frac{1}{\delta K} e^{\int_{T_{i-1}}^{T_i}(a_0(s)+b_0(s)q)ds-\sum_{n=1}^{d}\Phi_n(T_{i-1},T_i,a_n+b_nq,0)+y_n(T_{i-1})\Psi_n(T_{i-1},T_i,a_n+b_nq,0)} \\ =& e^{f_1(T_{i-1})+\sum_{n=1}^{d} y_n(T_{i-1})g_1(n,T_{i-1})}, \end{aligned}$$

where

$$f_1(T_{i-1}) = -\ln(\delta K) + \int_{T_{i-1}}^{T_i}(a_0(s) + b_0(s)q)ds - \sum_{n=1}^{d}\Phi_n(T_{i-1}, T_i, a_n + b_nq, 0), \quad (5.17)$$

$$g_1(n, T_{i-1}) = -\Psi_n(T_{i-1}, T_i, a_n + b_nq, 0), \quad (5.18)$$

and

$$e^{X_2(T_{i-1})} = \frac{1}{\delta K} \frac{1}{e^{-\int_{T_{i-1}}^{T_j}(a_0(s)ds+\sum_{n=1}^{d}(\Phi_n(T_{i-1},T_i,a_n,0)+y_n(T_{i-1})\Psi_n(T_{i-1},T_i,a_n,0))}} \quad (5.19)$$

$$= \frac{1}{\delta K} e^{\int_{T_{i-1}}^{T_j}(a_0(s))ds+\sum_{n=1}^{d}(\Phi_n(T_{i-1},T_i,a_n,0)+y_n(T_{i-1})\Psi_n(T_{i-1},T_i,a_n,0))} \quad (5.20)$$

$$= e^{f_2(T_{i-1})+\sum_{n=1}^{d} y_n(T_{i-1})g_2(n,T_{i-1})}, \quad (5.21)$$

where

$$f_2(T_{i-1}) = -\ln(\delta K) + \int_{T_{i-1}}^{T_i} a_0(s)ds - \sum_{n=1}^{d}\Phi_n(T_{i-1}, T_i, a_n, 0), \quad (5.22)$$

$$g_2(n, T_{i-1}) = -\Psi_n(T_{i-1}, T_i, a_n, 0). \quad (5.23)$$

Here the deterministic functions Φ_n, Ψ_n are defined by

$$\Phi_n(0, t, \mu, \alpha) = -\frac{2\theta_n\kappa_n}{\sigma_n^2}\ln\left(\frac{(\sigma_n^2\alpha + \kappa_n)(e^{\sqrt{A_n}t} - 1) + \sqrt{A_n}(e^{\sqrt{A_n}t} + 1)}{2\sqrt{A_n}e^{\frac{\sqrt{A_n}+\kappa_n}{2}t}}\right), \quad (5.24)$$

$$\Psi_n(0, t, \mu, \alpha) = \frac{(\alpha\kappa_n - 2\mu)(e^{\sqrt{A_n}t} - 1) - \alpha\sqrt{A_n}(e^{\sqrt{A_n}t} + 1)}{(\sigma_n^2\alpha + \kappa_n)(e^{\sqrt{A_n}t} - 1) + \sqrt{A_n}(e^{\sqrt{A_n}t} + 1)}, \quad (5.25)$$

with $A_n = \kappa_n^2 + 2\mu\sigma_n^2$.

In order to apply the argument of Hurd and Zhou (2010) on the pricing of spread options, we need to compute the joint characteristic function of (X_1, X_2). The conditional characteristic function of the random vector (X_1, X_2) defined in (5.11), (5.12) is given

Table 13: CIR model parameters — one–factor model ($d = 1$)

Model parameters	
κ	0.2703
θ	0.0434
σ	0.0272
a	0.2
b	0.2
q	0.6
a_0	0.2
b_0	0.2

by

$$\begin{aligned}\mathbb{E}_t^{\mathbb{Q}}\left[e^{\mathrm{i}(u_1X_1(T_{j-1})+u_2X_2(T_{i-1}))}\right] &= e^{\mathrm{i}(u_1f_1(T_{i-1})+u_2f(T_{i-1})}\mathbb{E}_t^{\mathbb{Q}}\left[e^{\mathrm{i}\sum_{n=1}^{d}y_n(T_{i-1})(u_1g_1(n,T_{i-1})+u_2g_2(n,T_{i-1}))}\right]\\ &= e^{\mathrm{i}(u_1f_1(T_{i-1})+u_2f(T_{i-1})+\sum_{n=1}^{d}\Phi_n(t,T_{i-1},0,-\mathrm{i}(u_1g_1(n,T_{i-1}))+u_2g_2(n,T_{i-1})))}\\ &\quad\cdot e^{\sum_{n=1}^{d}y_n(t)\Psi_n(t,T_{i-1},0,-\mathrm{i}(u_1g_1(n,T_{i-1})+u_2g_2(n,T_{i-1}))},\end{aligned}$$

where the deterministic functions f_1, f_2, g_1, g_2 are defined in (5.17)-(5.23). The transform is well defined for all $u_1, u_2 \in \mathbb{C}$ and for all $n = 1, ..., d$.

$$\Im[u_1g_1(n,T_{i-1}) + u_2g_2(n,T_{i-1})] \geq -\frac{2\kappa_n}{\sigma_n^2} \tag{5.26}$$

where $\Im$ denotes the imaginary part of a complex number.

Numerical example

Numerical results based on the parameter constellation in Table 13 are provided in Table 14. The Monte Carlo estimates and associated 95%–confidence intervals are based on 10 million simulations with 1000 time steps. $N = 2^{10}$ and $\bar{u} = 160$ are used for the FFT computation. In this case, we see that the lower bound approximation by integration of Caldana and Fusai (2013) gives a quite accurate result, outperforming FFT.

6 Concluding remarks

Building on the Fourier transform approach to pricing spread options of Hurd and Zhou (2010), we show that their result is in essence an application of the two–dimensional Parseval Identity. Implementing the method using the highly efficient FFTW C++ library, we clarify a little–documented issue in order to reconcile this implementation with the widely used Matlab *ifft2* function. We replicate the numerical results reported in Hurd

Table 14: LIBOR-OIS spread option prices, K taken to be the spot spread.

				Monte Carlo		
T	**K**	**FFT**	**Integration**	**Low bound**	**Price**	**Upper bound**
0.5	0.003383	0.070773	0.070706	0.070706	0.070706	0.070707
1.0	0.001660	0.163826	0.163977	0.163976	0.163977	0.163978
2.0	0.002300	0.162695	0.162698	0.162698	0.162698	0.162699
3.0	0.003400	0.161088	0.161078	0.161076	0.161077	0.161078
4.0	0.005070	0.158877	0.158946	0.158945	0.158945	0.158946
5.0	0.007100	0.156471	0.156514	0.156513	0.156514	0.156514
6.0	0.009278	0.410270	0.410338	0.410333	0.410335	0.410338
8.0	0.012389	0.148448	0.148444	0.148443	0.148444	0.148445
9.0	0.012504	0.146426	0.146363	0.146361	0.146362	0.146363
10.0	0.012240	0.143095	0.143059	0.143058	0.143058	0.143059

and Zhou (2010), and provide additional application examples, both in terms of models (NIG) and in terms of products (cross–currency and LIBOR/OIS interest rate spread options). All application examples are benchmarked against Monte Carlo simulation. The method proved to be fast and accurate even for coarser grids, in fact we obtained sufficiently accurate results with just $N = 2^8$ and integration limit of $\bar{u} = 40$, with the exception of the CIR–type model for the LIBOR/OIS spread, where we set $N = 2^{10}$ and $\bar{u} = 160$.

References

Alfeus, M., Grasselli, M. and Schlögl, E. (2017), 'A Consistent Stochastic Model of the Term Structure of Interest Rates for Multiple Tenors.', *SSRN Working paper* .
URL: *https://papers.ssrn.com/sol3/papers.cfm?abstract_id=2972428*

Black, F. and Scholes, M. (1973), 'The pricing of options and corporate liabilities', *The Journal of Political Economy* **81**(1), 637–654.

Brigo, D. and Mercurio, F. (2006), *Interest rate models-theory and pratice with smile, inflation and credit*, Springer finance, Berlin.

Caldana, R. and Fusai, G. (2013), 'A general closed-form spread option pricing formula', *Journal of Banking & Finance* **37**, 4893–4906.

Carr, P. and Madan, B. (1999), 'Option valuation using the fast Fourier transform', *The Journal of Computational Finance* **2(4)**.

Cox, J., Ingersoll, J. and Ross, S. (1985), 'A theory of the term structure of interest rates', Econometrica **53**(2), 385–407.

Dempster, M. and Hong, S. (2002), 'Spread option valuation and the fast Fourier transform', *in Mathematical Finance-Bachelier Congress 2000* pp. 203–220.

Eberlein, E., Glau, K. and Papapantoleon, A. (2010), 'Analysis of Fourier transform valuation formulas and applications', *Applied mathematical Finance* **17**, 211–240.

Frigo, M. and Johnson, S. (2010), 'FFTW user's manual', *MIT* .

Hurd, T. and Zhou, Z. (2010), 'A Fourier transform method for spread option pricing', *SIAM J. Financial Math.* **1(1)**, 142–157.

Kienitz, J. and Wetterau, D. (2012), *Financial Modelling: Theory, Implementation and practice (with Matlab source)*, 3rd Ed. John Wiley & sons Ltd.

Kirk, E. (1995), 'Correlation in the energy markets', *In Managing Energy Price Risk (First Edition). London: Risk Publications and Enron* pp. 71–78.

Lewis, A. (2001), 'A simple option formula for general jump-diffusion and other exponential Lévy processes', OptionCity.net publications .
URL: *http://optioncity.net/pubs/ExpLevy.pdf*

Luciano, E. and Schoutens, W. (2006), 'A multivariate jump-driven financial asset model', *Quantitative Finance* **6**(5), 385–402.

Mercurio, F. (2002), 'Pricing of Options on two Currencies Libor Rates', *Financial Models, Banca IMI* .
URL: *http://www.fabiomercurio.it/SpreadOptionLibor.pdf*

Schlögl, E. (2002), 'A multicurrency extension of the lognormal interest rate market models', *Finance and Stochastics* **6**(2), 173–196.

Sharma, V. and Dolas, P. D. (2016), 'Modulation and Parseval's theorem for distributional two dimensional Fourier-Mellin transform', *International Journal of engineering Science and Research Technology* **5**(8), 559–564.